



Infrared Radiance of Mount Etna, Sicily

MATTHEW BLACKETT

Department of Geography, Kings College, Strand, London, WC2R 2LS, UK; matthew.blackett@kcl.ac.uk

(Received 18th February 2007; Accepted 4th June 2007)

Abstract: Thermal and short-wave infrared images of Mount Etna, acquired using the ASTER sensor on-board the EOS Terra satellite, are presented. The data from the short-wave infrared (SWIR) channel is plotted as a three-dimensional surface map showing the spatial distribution of radiance emitted from the summit craters of the volcano. The utility of using short-wave infrared data in producing such maps, as opposed to using long-wave infrared data, lies in allowing individually active craters to be discerned and differences in their radiant emissions to be quantified. This is an improvement over purely qualitative findings which can be drawn from the use of visual or thermal infrared imagery (TIR) of the same surfaces. The additional advantage of using SWIR bands is that in some cases, the quantitative observations can be related to the physical processes occurring at the volcano at the time of acquisition, thereby negating the requirement for potentially dangerous field observations of actively erupting volcanoes. The utility of SWIR observations in monitoring the behaviour of active volcanoes is therefore confirmed.



1. Introduction

Mount Etna is a complex stratovolcano located in eastern Sicily, north of the city of Catania (Donegan and Flynn, 2004). As the mythical home to Vulcan, the God of Fire, Mount Etna has long been a source of both fascination and fear for the people of Sicily who live in its shadow. It has one of the world's longest documented records of activity dating back to 1500 BC and is one of relatively few volcanoes on Earth that erupts nearly continuously (GVP, 2007; Behncke and Neri, 2003).

Mount Etna currently consists of a central conduit and four active summit craters (Acocella and Neri, 2003). Its activity in recent years has included numerous dangerous explosive eruptions and inundating lava flows which have forced evacuations and resulted in damage to land and property. Furthermore, degassing and emissions of ash are common occurrences at the summit (GVP, 2007). Figure 1 displays a sketch map of the volcano's summit craters; these can be compared with the location of emissions from the respective summits which are displayed on the SWIR image of the region (Map B).

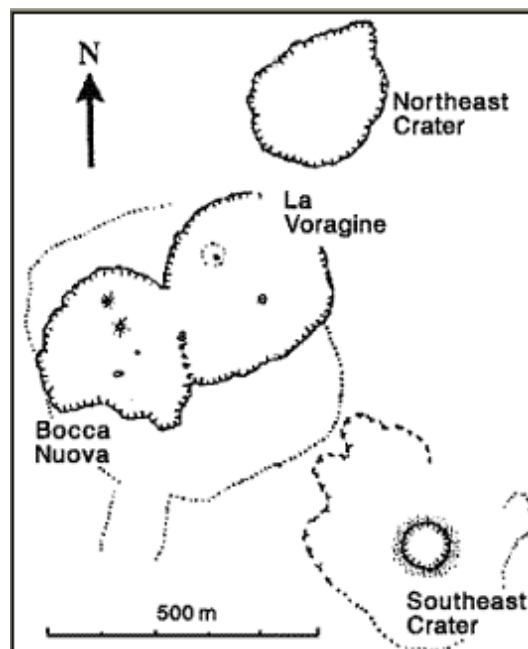


Figure 1. Field sketch of the craters at the summit of Mount Etna (adapted from Oppenheimer and Murray (1989)).

With the obvious perils associated with studying active volcanoes such as Mount Etna, it is clearly advantageous if they can be observed remotely. One way in which this is commonly conducted is through the use of satellite-mounted instruments. Due to the emissions of radiant energy associated with volcanic activity, infrared observations of active volcanoes have a particular utility in that they allow patterns of heat emission from a volcano to be imaged and quantified. These emissions relate directly to the processes occurring at the volcanic surface, and to some extent, within the volcano. Indeed, measurements of radiance emitted from a volcano have been used to determine lava effusion rates (Harris et al., 2000), discriminate various activity styles (Wooster et al., 2000) and collect long-term measurements of radiance trends useful for constructing simple process-based models of how a particular volcano functions (e.g. Wooster and Rothery, 1997). Radiance measurements can therefore, provide an indication of the status of a volcano without the need for potentially dangerous field visits.

All objects above 0 K (-273.15 °C) emit radiation. According to the Stefan-Boltzmann Law, the radiance that objects emit is proportional to the fourth power of their temperature and, according to Weins Displacement Law, the chief wavelength of emission becomes shorter as the object's temperature increases (Jensen, 2000). This effect is displayed in Figure 2. By virtue of the high temperatures often associated with active volcanic surfaces (which can be in excess of 1000 K) active volcanoes often emit significantly in the SWIR region of the electromagnetic spectrum. As such, SWIR imagery can be used to map these emissions, of which Map B is an example. Similar mappings are possible using TIR imagery (examples of which are displayed as Maps A and D) but its utility is reduced in relation to monitoring hot active volcanic summits due to the significantly lower TIR emissions from hot surfaces in comparison to that of SWIR bands, as is evident from Figure 2.

Radiance can be measured in units of Watts per square metre, per steradian, per unit wavelength ($Wm^{-2}sr^{-1}\mu m^{-1}$): this effectively quantifies the amount of radiation of a specific wavelength, per unit solid angle, that leaves a surface in a given direction, per unit area of that surface (Jensen, 2000). As might be expected, for any particular SWIR wavelength observation, the higher the radiance value, the hotter the emitting surface must be (assuming the hot surface fills the entire imaging pixel).

There are a number of satellite-mounted SWIR imaging sensors, many of

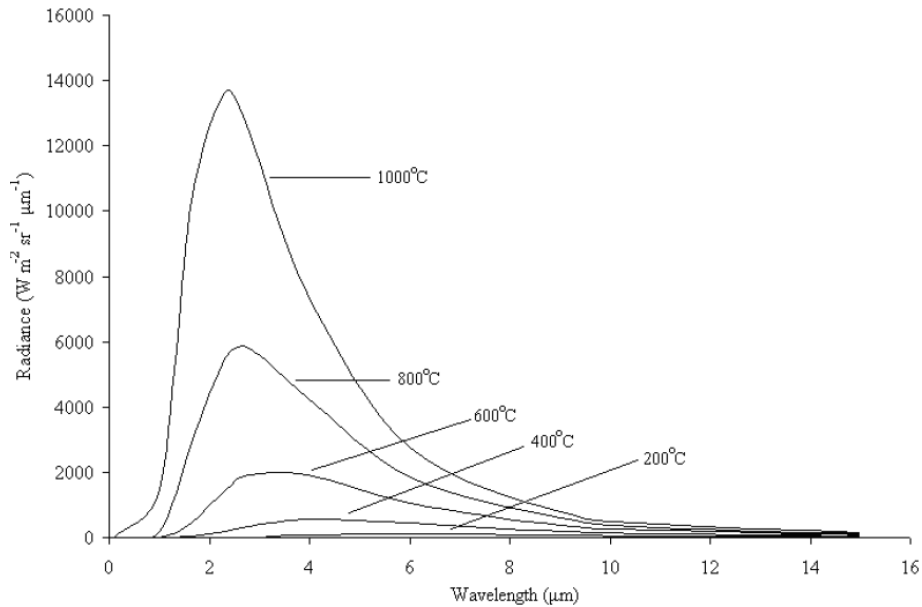


Figure 2. Depiction of the theoretical spectral radiance emitted from a surface at different temperatures, calculated using Planck's Radiation Law. Note: 1.) the decreasing wavelength of peak thermal emission with increasing temperature (Wein's Displacement Law) and 2.) the large increase in area under each curve (which represents the total energy emitted) with increasing temperature (the Stefan-Boltzmann Law).

which have been used to monitor active volcanic surfaces. One of the most sophisticated sensors currently in orbit is the Advanced Spaceborne Thermal Emission and Reflectance Radiometer (ASTER) on-board the NASA Terra satellite. It is imagery from this sensor that is examined in this work and used to map thermal emissions from the craters of Mount Etna.

2. Methods

2.1 Satellite Image Acquisition

The ASTER image of Mount Etna was obtained on the 23 July 2002 and distributed through the [NASA Earth Observation System Data Gateway](#). The image was acquired at night and contains data from both SWIR and TIR spectral bands. As the ASTER sensor has a repeat coverage of around 16-days, cloud-free observations of active volcanoes are relatively rare and as such, it is fortunate that such a clear image as this is available.

2.2 Satellite Image Processing

Initially, the data within each image was converted to values of radiance. This was conducted using the conversion equation and coefficients detailed in [Abrams et al. \(1999\)](#). Both the TIR and SWIR images were then analysed separately.

Thermal infrared image. The TIR image presented here (Map A) was obtained in ASTER band 10 ($8.275 \mu m$) which has a pixel size of 90 m and an overall scene size of 63 x 63 km. Map D shows the entire region from which the summit image, Map A, was taken. Each image was rotated to align it with North, and a latitude and longitude graticule was overlaid. Band 10 was chosen due to the clarity of the scene acquired using this band.

Short-wave infrared image. In contrast to TIR imagery, night-time imagery in SWIR bands often appears noisy since, away from the volcano, the detected signal is attributable to that from the instrument itself (the ambient ground surface being too cold to emit at these wavelengths; see Figure 2). The SWIR image presented here (Map C) was obtained in ASTER band 9 ($2.395 \mu m$) which has a pixel size of 30 m. It is shown prior to the application of a noise removal procedure. This image has also been arbitrarily contrast stretched to increase the visibility of the anomalous areas over the background noise. It can be troublesome to remove the effects of background noise completely so as to leave simply the radiant signal associated with the thermally anomalous volcanic surface. For the purposes of this article, the background noise was quantified by selecting a region of the SWIR image adjacent to the volcano and determining its mean. This mean was then subtracted from the data of the whole image to leave, primarily, just the signal associated with the thermally anomalous volcanic surface. Such a noise subtraction process is relatively standard practice ([Wooster and Rothery, 1997](#)).

2.3 3-D Thermal Mapping Procedure

All thermally anomalous signals remaining after the subtraction of the background noise were entered as a two-dimensional array into the IDL programming environment and graphed as a three-dimensional surface (Figure 3). This figure highlights the quantitative variations in radiance

over the volcanic surface. The surface created is outlined in red so as to highlight its areal extent; the same red outlined region is depicted in Maps A, B and D.

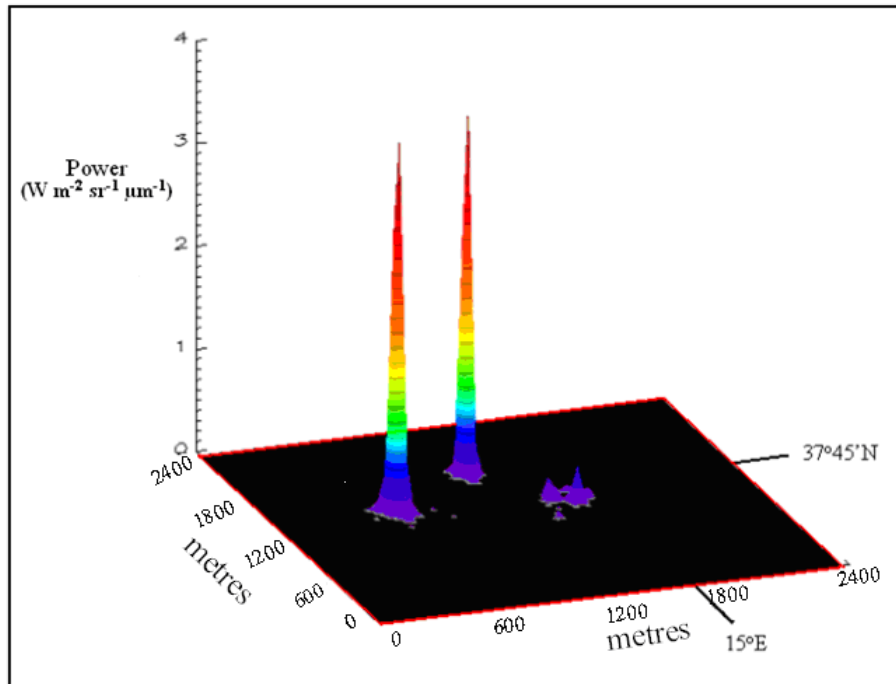


Figure 3. A three-dimensional representation of the SWIR radiance emitted from the summit crater of Mount Etna, taken from the data displayed in Map B.

3. Conclusions

The SWIR radiance map (Map B) and 3-D surface plot (Figure 3) clearly show three radiance peaks, each associated with one of the crater regions of Mount Etna. The three peaks relate, from north to south, to the Northeast crater, the La Voragine and Bocca Nuova crater complex and the Southeast crater and can be correlated with the sketch map of the summit (Figure 1).

It appears that the radiant emissions from the northeast crater and the La Voragine and Bocca Nuova crater complex are significantly higher than those of the southeast crater. This observation can be related to the volcanic activity occurring at the time. During this period, Mount Etna was displaying moderate activity characterised by prolonged emissions of

ash and gases from Bocca Nuova, and the presence of cooling lava bombs within the Northeast crater following previous explosions and accompanied by intense steam emissions. During the same period, the Southeast Crater showed virtually no activity with only weak gas emissions (BGVN, 27:08, 08/2002). The SWIR image (Map B) and the 3D surface (Figure 3) reflect these volcanic processes, providing a realistic indication of the activity levels within each crater. The same features are less apparent in the TIR image of the same surface (Map A) due to the reduced sensitivity of the TIR bands to such hot surfaces (see Figure 1) and also, due to the larger pixel size of the TIR instrument.

The utility of satellite-derived radiance imagery is apparent, particularly in the case of SWIR imagery, providing a reliable indication of the processes occurring within a volcanic complex without the risks associated with field observation. Such imaging is also useful not only in mapping spatial variations in radiant emissions but also, if collected over time, any temporal variations might provide indications as to the longer-term trends in the behaviour of any volcanoes being examined.

Acknowledgements

Thanks are due to my PhD Supervisor, Professor Martin Wooster, for setting aside research funding to purchase the scene examined in this work.

Software

Satellite imagery was viewed and manipulated using ENVI 4.3 and the radiance surface map was produced using IDL 6.3.

References

- ABRAMS, M., HOOK, S. and RAMACHANDRAN, B. (1999) ASTER User Handbook, Version 2, Tech. rep., NASA/Jet Propulsion Laboratory, Pasadena.
- ACOCELLA, V. and NERI, M. (2003) What makes flank eruptions? The 2001 Etna eruption and its possible triggering mechanisms, *Bulletin of Volcanology*, 65, 517–529.
- BEHNCKE, B. and NERI, M. (2003) Cycles and trends in the recent eruptive behaviour of Mount Etna (Italy), *Canadian Journal of Earth Science*, 40, 1405–1411.
- BGVN (2002) Global Volcanism Network. Etna. Smithsonian Institute, *Bulletin of the Global Volcanism Network*, 27:08, 08/2002.
- DONEGAN, S. and FLYNN, L. P. (2004) Comparison of the response of the Landsat 7 Enhanced Thematic Mapper + and the Earth Observing-1 Advanced Land Imager over active lava flows, *Journal of Volcanology and Geothermal Research*, 135, 105–126.
- GVP (2007) Global Volcanism Program. Etna Summary, [online]. Available from:
<http://www.volcano.si.edu/world/volcano.cfm?vnum=0101-06=>
[Last accessed: 21 January, 2007].
- HARRIS, A. J. L., FLYNN, L. P., DEAN, K., PILGER, E., WOOSTER, M., OKUBO, C., MOUGINIS-MARK, P., GARBIEL, H., THORNER, C., DE LA CRUZ-REYNA, S., ROTHERY, D. and WRIGHT, R. (2000) Remote sensing of active volcanism, chap. Real-time satellite monitoring of volcanic hot spots, *AGU Geophysical Monograph* 116, pp. 139–159.
- JENSEN, J. R. (2000) *Remote Sensing of the Environment. An Earth Resource Perspective*, Prentice Hall, Saddle River, NJ.
- NASA EARTH OBSERVATION SYSTEM DATA GATEWAY (2007) [Online]. Available from:
<http://edcimswww.cr.usgs.gov/pub/imswelcome/>, [Last accessed: 4 June, 2007].
- OPPENHEIMER, C. and MURRAY, J. (1989) Field sketch in Seismic Event, *Alert Network Bulletin*, 14:07.

WOOSTER, M. J., KANEKO, T., NAKADA, S. and SHIMIZU, H. (2000) Discrimination of lava dome activity styles using satellite derived thermal structures, *Journal of Volcanology and Geothermal research*, 102, 97–118.

WOOSTER, M. J. and ROTHERY, D. A. (1997) Thermal monitoring of Lascar Volcano, Chile, using infrared data from the along-track scanning radiometer: a 1992-1995 time series, *Bulletin of Volcanology*, 58, 566–579.